https://doi.org/10.5194/acp-2020-461
Preprint. Discussion started: 2 June 2020

Atmospheric Chemistry and Physics Discussions

Influence of aromatics on tropospheric gas-phase composition

Domenico Taraborrelli[1], David Cabrera-Perez[2], Sara Bacer[2,*], Sergey Gromov[2], Jos Lelieveld[2], Rolf Sander[2], and Andrea Pozzer[2,3]

[1]Institute of Energy and Climate Research (IEK-8), Forschungszentrum Jülich GmbH, 52425 Jülich, Germany
[2]Atmospheric Chemistry Department, Max-Planck Institute of Chemistry, Hahn-Meitner-Weg 1, 55128 Mainz, Germany
[3]International Centre for Theoretical Physics, 34100 Trieste, Italy
[*]Now at: Université Grenoble Alpes, CNRS, Grenoble INP, LEGI, 38000 Grenoble, France

Correspondence: D. Taraborrelli (d.taraborrelli@fz-juelich.de)

Abstract.

Aromatics contribute a significant fraction to organic compounds in the troposphere and are mainly emitted by anthropogenic activities and biomass burning. Their oxidation in lab experiments is known to lead to the formation of ozone and aerosol precursors. However, their overall impact on tropospheric composition is uncertain as it depends on transport, multiphase chemistry, and removal processes of the oxidation intermediates. Representation of aromatics in global atmospheric models has been either neglected or highly simplified. Here, we present an assessment of their impact on the gas-phase chemistry, using the general circulation model EMAC (ECHAM5/MESSy Atmospheric Chemistry). We employ a comprehensive kinetic model to represent the oxidation of the following monocyclic aromatics: benzene, toluene, xylenes, phenol, styrene, ethylbenzene, trimethylbenzenes, benzaldehyde, and lumped higher aromatics that contain more than 9 C atoms.

Significant regional changes are identified for several species. For instance, glyoxal increases by 130 % in Europe and 260 % in East Asia, respectively. Large increases in HCHO are also predicted in these regions. In general, the influence of aromatics is particularly evident in areas with high concentrations of NO_x, with increases up to 12 % in O_3 and 17 % in OH.

On a global scale, the estimated net changes are minor when aromatic compounds are included in our model. For instance, the tropospheric burden of CO increases by about 6 %, while the burdens of OH, O_3, and NO_x ($NO + NO_2$) decrease between 3 % and 9 %. The global mean changes are small, partially because of compensating effects between high- and low-NO_x regions. The largest change is predicted for the important aerosol precursor glyoxal, which increases globally by 36 %. In contrast to other studies, the net change in tropospheric ozone is predicted to be negative, -3 % globally. This change is larger in the northern hemisphere where global models usually show positive biases. We find that the reaction with phenoxy radicals is a significant loss for ozone, of the order of 200-300 Tg/yr, which is similar to the estimated ozone loss due to bromine chemistry.

Although the net global impact of aromatics is limited, our results indicate that aromatics can strongly influence tropospheric chemistry on a regional scale, most significantly in East Asia. An analysis of the main model uncertainties related to oxidation and emissions suggests that the impact of aromatics may even be significantly larger.

Changes of what?

Is this a net loss? If not, is it a very important finding?

https://doi.org/10.5194/acp-2020-461
Preprint. Discussion started: 2 June 2020

Atmospheric Chemistry and Physics Discussions

1 Introduction

Volatile organic compounds (VOCs) comprise a large variety of species which influence the tropospheric chemistry at local, regional, and global scales. VOCs react mainly with the hydroxyl radical (OH), ozone (O_3), and the nitrate radical (NO_3), or they are photolyzed. Their oxidation affects many key atmospheric species, including OH, O_3, and nitrogen oxides (NO_x = NO + NO_2). Production and destruction of ozone are controlled by the ratio of VOCs to NO_x. In the low-NO_x regime, the net effect of VOC oxidation is ozone destruction. Under high-NO_x conditions, e.g., in urban areas, O_3 is generated by the oxidation of VOCs (Sillman et al., 1990).

Is

L31: This is too vague. There are specific definitions of aromaticity with implications for the chemistry of compounds in this class.

Aromatics are a subset of unsaturated organic compounds of which several are present in the atmosphere, e.g., benzene, toluene, ethylbenzene, xylenes, styrene and trimethylbenzenes. In general, aromatic compounds are found in continental areas, especially in industrialized urban and semi-urban regions (Barletta et al., 2005) where their emissions are highest. They are responsible for a considerable fraction of ozone and secondary organic aerosol (SOA) formation (Ng et al., 2007; Lee et al., 2002; Ran et al., 2009). In addition, many aromatics are toxic (WMO, 2000).

Emissions of aromatics are primarily anthropogenic, related to fuel combustion, and leakage from fuels and solvents (Koppmann, 2007; Sack et al., 1992). Emissions from biomass burning play a secondary role but can be important on a regional scale (Cabrera-Perez et al., 2016). Biogenic emissions are only relevant for toluene, although recent studies suggest that other aromatics from biogenic sources may rival those from fossil fuel use (Misztal et al., 2015).

L38: Add a reference for the toluene biogenic emissions.

As shown by Cabrera-Perez et al. (2016), aromatic compounds are removed from the atmosphere mainly via chemical oxidation. Dry deposition is a minor sink, and wet deposition is almost negligible. The gas-phase chemistry of aromatics has been the subject of many studies (e.g., Atkinson et al., 1989; Warneck, 1999; Koppmann, 2007). Due to their high reactivities, aromatics have relatively short atmospheric lifetimes ranging from hours to a few days. Their oxidation is mainly controlled by the OH radical but they also react with NO_3 and O_3. The reaction with OH can proceed along two principal pathways. The first starts with H-abstraction from an aliphatic substituent. The following reactions are similar to those of aliphatic compounds and involve the addition of O_2, yielding a peroxy radical as an intermediate. Toluene, for example, can be oxidized in this way to benzaldehyde. The second, which is the dominant path, is OH addition to the aromatic ring. Secondary reactions can lead to ring opening and complex further reactions, eventually generating HCHO, glyoxal, and other smaller organic molecules. The products from the oxidation of aromatic compounds have a reduced volatility and allow for the formation of SOA, which in turn can significantly reduce the gas-phase concentrations of the aromatic oxidation products.

L42: Is that true of all aromatics? i.e. benzene?

Numerical models are essential to understand the highly complex chemical degradation of aromatics and to quantify the impact of these compounds in atmospheric chemistry. A very detailed modeling of aromatics is possible with the reactions contained in the Master Chemical Mechanism (MCM, Jenkin et al., 2003). However, due to its complexity, the full mechanism is mainly suitable for box model calculations. For global studies, simplified reaction schemes are usually used (e.g., Emmons et al., 2010; Hu et al., 2015).

The main objective of this study is to investigate how tropospheric OH, O_3, NO_x, and several VOC concentrations are affected by the oxidation of several monocyclic aromatics. The paper is organized as follows. In Sect. 2, the numerical model

L46-50: There is a rich literature on many aspects of this chemistry which should be cited.

https://doi.org/10.5194/acp-2020-461
Preprint. Discussion started: 2 June 2020

Atmospheric Chemistry and Physics Discussions

and the set-up of the simulations are described. Section 3 analyzes the calculated impact on selected chemical species both on the global and on the regional scales.

2 Model description

We used the ECHAM5/MESSy Atmospheric Chemistry (EMAC) model, which is a numerical chemistry and climate simulation system that includes submodels describing tropospheric and middle atmosphere processes (Jöckel et al., 2010). EMAC uses the second version of the Modular Earth Submodel System (MESSy2) to link multi-institutional computer codes. The core atmospheric model is the 5th generation European Centre Hamburg general circulation model (ECHAM5, Roeckner et al., 2006).

For the present study we performed simulations with EMAC (ECHAM5 version 5.3.02, MESSy version 2.53) in the T63L31ECMWF resolution, which corresponds to a grid with a horizontal cell size of approximately $1.875° \times 1.875°$ and 31 vertical hybrid pressure levels, extending from the surface up to about 10 hPa.

Emission rates of the individual aromatics are shown in Tab. 1. The sum of all sources is 29.4 $\mathrm{TgC/a}$. For anthropogenic emissions, we used EDGAR 4.3.2 (Huang et al., 2017), distributed vertically as in Pozzer et al. (2009). The MESSy submodel MEGAN calculates biogenic emissions (Guenther et al., 2012). For biomass burning, the submodel BIOBURN was used, which integrates the Global Fire Assimilation System (GFAS) inventory (Kaiser et al., 2012).

Atmospheric chemistry was calculated with the MECCA submodel, which has been evaluated by Pozzer et al. (2007) and Pozzer et al. (2010). The most recent model version has been described by Sander et al. (2019). The mechanism for aromatic species is a reduced version of the MCM (Bloss et al., 2005b), as described in detail by Cabrera-Perez et al. (2016). In this study, we consider several additions to the MCM reactions:

- For several nitrophenols (MCM names: HOC6H4NO2, DNPHEN, TOL1OHNO2, MNCATECH, DNCRES), their photolysis reactions were added (Bejan et al., 2006), e.g.: L78: How were they added? i.e. what cross-sections and quantum yields used?

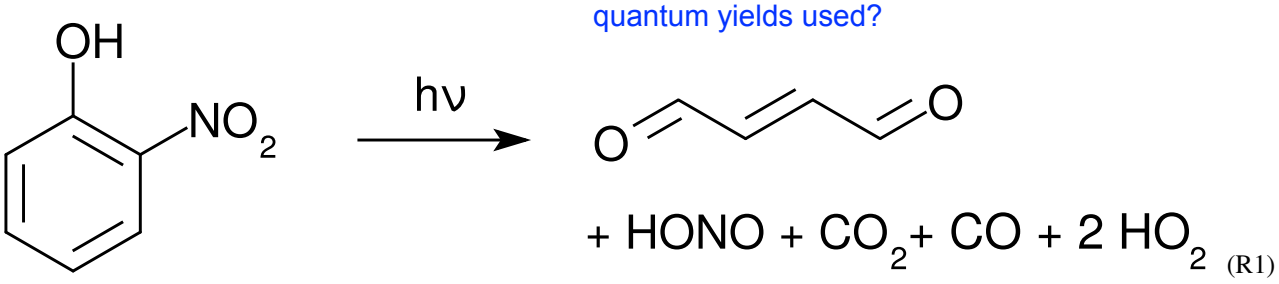

(R1)

- For the photolysis of benzaldehyde, the MCM uses the rate constant (j-value) of methacrolein as a proxy. We have calculated the j-value based on the UV/VIS spectrum of benzaldehyde recommended by Wallington et al. (2018). In our code, the photolysis of benzaldehyde produces $C_6H_5O_2$, HO_2 and CO.

https://doi.org/10.5194/acp-2020-461
Preprint. Discussion started: 2 June 2020

Atmospheric Chemistry and Physics Discussions

– For several phenyl peroxy compounds (MCM names: C6H5O2, CATEC1O2, OXYL1O2, MCATEC1O2, NCRES1O2), their reactions with NO_2 were added (Jagiella and Zabel, 2007), e.g.:

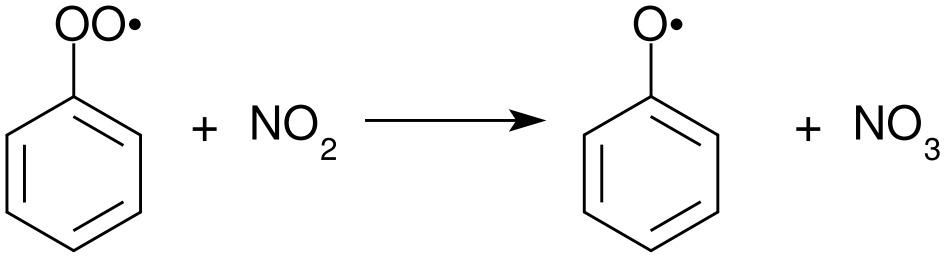

(R2)

– For the reaction of HO_2 with the peroxy radical C6H5CO3 (resulting from the oxidation of benzaldehyde), we use the yields provided by Roth et al. (2010).

– Alkyl nitrate yields are calculated as a function of temperature and pressure, as described by Sander et al. (2019).

– Bicyclic peroxy radicals in the oxidation mechanism of toluene produce some glyoxal and methyl glyoxal as suggested by Birdsall et al. (2010). Benzene is treated analogously.

L89: Please be quantitative.

The aerosol calculations follow the approach of Pringle et al. (2010), with the notable difference of the inclusion of the explicit organic aerosol submodel ORACLEv1.0 by Tsimpidi et al. (2014). Although, similar to Tsimpidi et al. (2014), low- and intermediate volatiles are parameterized as lumped species, the equilibrium with their equivalent aerosol phase is explicitly calculated for $\simeq$ 600 volatile organic carbon tracers via ORACLE. The volatility and the enthalpy of vaporization of each tracer is estimated with the approaches of Li et al. (2016) and Epstein et al. (2010), respectively.

The simulated period covers the years 2009–2010, with the first year as spin-up, and the year 2010 being used for the analysis. The feedback between radiation and chemistry was decoupled to avoid any influence of chemistry on the dynamics (QCTM mode by Deckert et al. (2011)). As a consequence, every simulation discussed here has the same meteorology, i.e., binary identical transport.

To analyze the influence of the aromatic compounds on atmospheric chemistry and composition, we performed three model simulations, as listed in Tab. 2. The *AROM* simulation includes all chemical reactions and emissions of the following monocyclic aromatic compounds: benzene, toluene, xylenes (lumped), phenol, styrene, ethylbenzene, trimethylbenzenes (lumped), benzaldehydes, and higher aromatics (as representative of aromatics with more than 9 carbon atoms). The reference simulation (*NOAROM*) is identical to *AROM*, except that it excludes aromatic compounds. In the *ONLYMCM* run, we reverted the additions and changes to the MCM that have been described above. Our focus is to compare *AROM* with *NOAROM*. Results of *ONLYMCM* are mainly interesting for benzaldehyde and HONO. As EMAC uses terrain-following vertical hybrid pressure coordinates, we will refer to "surface" as the lowest model level, with an average thickness of roughly 60 m.

https://doi.org/10.5194/acp-2020-461
Preprint. Discussion started: 2 June 2020

Atmospheric Chemistry and Physics Discussions

3 Results and discussion

L110: Please plot the data in nmol/mol to make things clearer for the reader.

Globally averaged surface mixing ratios obtained from all model simulations (*AROM*, *NOAROM*, and *ONLYMCM*) are listed in Tab. 3. Figure 1 shows the annual average mixing ratios of the sum of all aromatic compounds included in the simulation *AROM*. They are higher in continental areas and close to the surface. The highest values are predicted in the northern hemisphere (NH), in particular, in East and South Asia, as well as in parts of Europe, Africa, and the US, reaching up to about 1 $\mathrm{nmol/mol}$. The background mean mixing ratios in oceanic areas of the southern hemisphere (SH) are of the order of a few $\mathrm{pmol/mol}$. For a more detailed analysis, we have selected the following five regions, as defined in Figure 2: Amazon area (AMA), central Africa (CAF), eastern Asia (EAS), Europe (EUR), and eastern US (EUS). The budgets of selected chemical species were calculated within these regions (Tab. 5).

3.1 Hydroxyl radical (OH)

L118: Insert “surface” between these two words.

Figure 3 shows the model-calculated OH in the *AROM* and *NOAROM* simulations. When aromatics are introduced to the model, the global average concentration of OH decreases for two reasons: first, the direct reaction with aromatics consumes OH, and second, additional CO resulting from the degradation of aromatics represents an increased sink for OH. However, in eastern Asia, Europe, and the east coast of the US, where $\mathrm{NO_x}$ concentrations are high, an increase of OH can be seen. Although the aromatics decrease $\mathrm{NO_x}$ in these areas (see below), the chemical system remains in the high-$\mathrm{NO_x}$ regime.

We find a positive correlation between OH and anthropogenic emissions in these regions but a negative correlation in the low-$\mathrm{NO_x}$ CAF region. The increased OH in the high-$\mathrm{NO_x}$ regions is mainly caused by the reaction of NO with $\mathrm{HO_2}$.

Figure 4 shows the seasonal cycle of the OH mixing ratio in the planetary boundary layer for the NH and SH. Inclusion of the aromatics leads to a relative decrease between 2.5 % and 5.5 %. Higher OH concentrations are identified over continental areas during the NH autumn, winter and spring than in summer (Fig. 3). In summer, OH concentrations increase only at a few locations when aromatics are included.

Figure 5 shows the annual zonal mean changes of the OH mixing ratio. The changes are most pronounced in the NH upper troposphere where reductions range from 7 % to 20 %. This helps bringing the model-simulated inter-hemispheric OH asymmetry closer to that derived from observations (Lelieveld et al., 2016). Globally, aromatics oxidation reduces OH by 7.7 % and consequently increases methane lifetime.

L131-132: Can you be more specific on both the impact on the OH NH:SH ratio change and the impact on the methane lifetime.

3.2 Ozone ($\mathrm{O_3}$)

In most areas of the globe, surface ozone is slightly lower in *AROM* than in *NOAROM* (Fig. 6). The $\mathrm{O_3}$ reduction is due to (i) the decrease in $\mathrm{NO_x}$ concentrations (limiting ozone formation) and (ii) increasing radical production (OH, $\mathrm{HO_2}$, and $\mathrm{RO_2}$) in ozone-depleting regimes, which enhances reactions of $\mathrm{O_3}$ with $\mathrm{HO_2}$ and OH. Only a few high-$\mathrm{NO_x}$ regions, where hydrocarbons are the limiting factor for ozone formation, show increased ozone concentrations: mainly East China (EAS), but also the eastern US (EUS) and Europe (EUR). The increases in these areas correlate with anthropogenic emissions of

L135-136: Has there been an increase in the flux through O3+OH? I’m surprised given the OH has gone down in these regions.

https://doi.org/10.5194/acp-2020-461
Preprint. Discussion started: 2 June 2020

Atmospheric Chemistry and Physics Discussions

L153: Can you confirm which definition you used in the analysis?

L141: Odd to ref. Fig 9 before 7 or 8. Re-order?

aromatics, which have significant ozone formation potentials. We find a positive correlation between O_3 and anthropogenic emissions in the EAS and EUR regions but a negative correlation in the low-NO_x CAF region.

The seasonal cycles of the relative differences show lower amplitude than for OH, but similar patterns (Fig. 9). The impact of aromatics is smallest in summer.

The zonal mean changes of O_3 mixing ratio in the troposphere are uniformly negative (Fig. 7). Similar to surface ozone, the annual mean changes for *ONLYMCM* and *AROM* are $-2.3\,\%$ and $-3.0\,\%$, respectively. The hemispheric changes are shown in Tab. 4. It is well known that MCM for aromatics overestimates ozone production in chamber experiments (Bloss et al., 2005b). The issue has been analysed in the companion paper (Bloss et al., 2005a) where the best mechanism improvement was found to be an early OH source during oxidation. Cabrera-Perez et al. (2016) introduced enhanced HO_x-sources by photolysis of benzaldehyde and nitrophenols. These modifications consistently result in less ozone produced with respect to MCM. These results deviate from the results by Yan et al. (2019) who suggested a global increase of 0.4 % due to aromatics. However, they only considered benzene, toluene and xylenes. Our results, obtained with a more comprehensive setup, suggest that aromatics could slightly ameliorate the model overestimate in the NH (Jöckel et al., 2016; Young et al., 2018). The overall tropospheric ozone burden decreases from 381 to 369 Tg for the *AROM* simulation. These estimated changes are robust against the tropopause definition and are about -3.5 and -2.3 % for the Northern and Southern Hemispheres, respectively (Table 4). These changes are associated with the enhanced direct ozone loss by reactions with organic compounds. It is widely acknowledged that this direct loss is only due to the ozonolysis of unsaturated VOCs and is estimated to be about 100 $\mathrm{Tg/yr}$, less than 2 % of the tropospheric ozone budget (Tilmes et al., 2016). However, with aromatics a new direct ozone loss process involving organic radicals comes in place. In Figure 8 the change in tropospheric ozone burden is shown against the change in ozone loss with organic compounds. This change is estimated to be globally in the 200-300 Tg/yr range depending on the mechanism used and is comparable to the loss by bromine chemistry in the troposphere (Sherwen et al., 2016)). Ozone is known to react with organic radicals like methyl peroxy radical although this loss is an insignificant sink (Tyndall et al., 1998). We find that phenoxy radicals from aromatics are a significant sink term of ozone ($>$200 $\mathrm{Tg/yr}$). These radicals are unique to aromatics oxidation and they also react with NO and NO_2. When the concentrations of NO_x are relatively low, C_6H_5O has sufficiently long lifetime to react with O_3. This ozone loss is modelled based on the results by Tao and Li (1999) for phenoxy radical

L155: Is it widely acknowledged that it is "only" ozonolysis? And does the definition of loss change with different constructs of the O3 budget (c.f. Bates and Jacob 2019)?

L156: Perhaps add e.g., as this is just one models calculation.

L161: Confirm if you mean ozone or odd-oxygen?

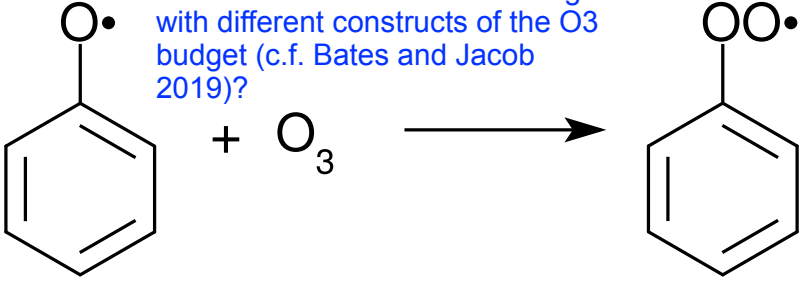

(R3)

https://doi.org/10.5194/acp-2020-461
Preprint. Discussion started: 2 June 2020

Atmospheric Chemistry and Physics Discussions

This ozone loss is enhanced by phenoxy radical production in the R2 reaction and the subsequent loss of odd oxygen by NO_3 photolysis and N_2O_5 heterogeneous loss

L166-167: Can you quantify the relative contribution of these different pathways to the 200 Tg/yr O3 (odd oxygen?) loss?

$$NO_3 + h\nu \rightarrow NO + O_2 \quad \text{(R4)}$$

$$NO_3 + NO_2 \rightarrow N_2O_5 \quad \text{(R5)}$$

$$N_2O_5 + H_2O \rightarrow 2HNO_3(aq) \quad \text{(R6)}$$

L174: But the way you have written R1 suggests that phenoxy radicals are not formed (instead butenedial is formed).

In our chemical kinetics mechanism (also in MCM) the reaction system just described constitutes an effective catalytic destruction cycle of odd oxygen. The strength of this cycle depends on the phenoxy radical levels and is significantly reduced in *AROM* compared to *onlyMCM* (Figure 8). We ascribe this difference to MCM not accounting for the photolysis of nitrophenols (R1) as determined by Bejan et al. (2006) preventing reformation of phenoxy radicals.

Our results for ozone differ both in magnitude and sign compared to the global study by Yan et al. (2019). However, the latter used the SAPRC-11 oxidation mechanism (Carter and Heo, 2013) which does not account for the reaction of phenoxy radicals with ozone (R3) and phenylperoxy radicals with NO_2 (R2).

3.3 Inorganic nitrogen

The simulated annual mean NO_x concentrations at the surface are significantly lower in *AROM* than in *NOAROM* (Figs. 10 and 11). One reason is the formation of aromatic species containing nitrogen (e.g., nitrophenols) in *AROM*, thereby transferring part of the NO_x burden to the nitrogenated species. The largest decreases (both absolute and relative) are found in regions with high NO_x concentrations. Since the ozone chemistry is not NO_x-limited in these regions, the impact on ozone is small. This holds for the free troposphere for which zonal average decreases in NO_x can be larger than 20 % (not shown), which in turn significantly influence OH (Fig. 5).

On the one hand, the reaction with aromatics is a sink for NO_3. On the other hand, NO_3 is produced in the phenylperoxy reaction with NO_2 (R2). Comparing *AROM* to *NOAROM*, the global average of the nighttime species NO_3 increases by more than 7 % (Tab. 3). In contrast to the global mean tendency, NO_3 decreases in several regions in Africa, South America, and India (Fig. 12). These decreases correlate well with emissions from biomass burning.

Although the net change of global HONO is small (about 3 % less in *AROM* than in *NOAROM*, see Figure 13 and Tab. 3), the regional differences can be large (Tab. 5). A decrease of HONO is seen mainly in polluted areas (EAS, EUR, EUS) in the winter. In contrast, HONO increases in the regions with emissions from biomass burning (AMA, CAF). Here, HONO is formed by the photolysis of nitrophenols (R1). Since these reactions are not included in the MCM, we do not see any HONO increase in the *ONLYMCM* simulation (Fig. 14).

On a global average level, HNO_3 is not affected much by aromatics. However, an increase can be seen in the regions where ozone increases (EAS) or where biomass burning decreases NO_3 and N_2O_5 (CAF), see Figure 15 and Tab. 5. An average zonal mean change of up to 5% throughout the UT/LS is linked to the enhanced NO_3 production by R2.

https://doi.org/10.5194/acp-2020-461
Preprint. Discussion started: 2 June 2020


Atmospheric Chemistry and Physics Discussions

3.4 Selected oxygenated compounds

Globally, HCHO is not affected much by aromatics. There are, however, regional differences. We find maximum absolute depletions in the AMA region, where concentrations are typically high (Fig. 16). Increased values of HCHO are mainly seen in EAS and EUR (Tab. 5).

α-dicarbonyls like glyoxal and methyl glyoxal are primarly produced from the bicycloalkyl-radical pathway leading in the case of benzene to BZBIPERO2 (MCM) (Volkamer et al., 2001). A minor secondary formation pathway from conjugated unsaturated dicarbonyls, e.g., MALDIAL (MCM), is also known and taken into account (Bloss et al., 2005b). As expected, the model predicts a very large increase of glyoxal in almost all continental areas (Figs. 17 and 18). The global burden is 36 % higher than in the *NOAROM* model simulation. The largest regional increases are in the EAS and EUR regions (Tab. 5). An exception to the global trend is the AMA region, where OH is too low to produce either glyoxal or methyl glyoxal. Annual mean increases exceed 50 % over the continents close to the surface. In the lower troposphere, zonal mean increases are in the 10-20 % range. These changes are of significance for the model SOA budget since these two dicarbonyls are estimated to produce a large fraction of SOA by cloud processing (Lin et al., 2012).

Comparing *AROM* to *ONLYMCM*, benzaldehyde decreases by more than 50 % when the photolysis rate constant (j-value) from the MCM (based on methacrolein) is replaced by our value (based on the UV/VIS spectrum of benzaldehyde). The more realistic photolysis rate enhances the production of radicals like HO_2.

Since additional reactive carbon compounds have been introduced in the model, the oxidation of aromatics produces more CO, which has a lifetime of about 1-3 months (Lelieveld et al., 2016). CO can travel long distances from its source, although its lifetime is not long enough to allow it to cross hemispheres (Daniel and Solomon, 1998). CO concentrations generally increase on the global scale, indicating a small addition to the carbon budget. When comparing *AROM* to *NOAROM*, we find an increase of about 6 % in the atmospheric burden of CO. Interestingly, maximum zonal average increases of 10-20 % (not shown) are found for the NH upper troposphere/lower stratosphere (UTLS) region.

4 Model uncertainties

The model calculations presented in this work are associated with some uncertainties related to the oxidation kinetic model and emissions. Gas-phase oxidation of aromatics is complex and the kinetic mechanism used in this study reflects the state of knowledge, advancements and limitations in the mechanism have recently been discussed (Vereecken, 2019). Recent progress has focused in particular on the source strength of aerosol precursors and not on the overall radical production which also affects ozone. Nevertheless, our kinetic model makes use of only one rate constant for the reaction R3 of phenoxy radicals with ozone (Tao and Li, 1999). It also assigns this rate constant to the substituted phenoxy radicals other than C_6H_5O. Unfortunately, there is only one study of the rate constant of R3 at 298 K. Although the 2-σ reported uncertainty is slightly larger than 10 %, the rate constant of 2.86×10^{-13} $cm^3\,molecules^{-1}\,s^{-1}$ has to be regarded as a lower limit. On the other hand, experimental evidence for the product of R3, being phenyl peroxy radical ($C_6H_5O_2$), has not been found although it was expected. If the products are different, then the catalytic O_3-destruction cycle illustrated in Sec. 3.2 would not be in place. However, a significant amount

https://doi.org/10.5194/acp-2020-461
Preprint. Discussion started: 2 June 2020


Atmospheric Chemistry and Physics Discussions

of ozone loss via R3 and analogous reactions is to be expected. Moreover, the ozone loss is likely underestimated because of the model not accounting for the photolysis of nitrophenols reforming phenoxy radicals. Different from the HONO-formation channel, which destroys the aromatic ring, channels yielding substituted phenoxy radicals may dominate (Cheng et al., 2009; Vereecken et al., 2016) and thus enhance ozone loss.

Cloud chemistry of organic compounds is known to suppress gas-phase HO_x-production and directly consume ozone (Lelieveld and Crutzen, 1990). The overall effect on ozone depends on the local chemical regime. In our study water-soluble products are set to only undergo wet deposition (dissolution and removal by precipitation). Their aqueous-phase chemistry might however have a non-negligible effect on ozone and other oxidants. For instance, phenol is known to react very quickly with OH in the aqueous-phase (Field et al., 1982). Moreover, phenoxide anions from phenols react quickly with ozone (Hoigné and Bader, 1983). In particular, nitrophenols might be efficient ozone scavengers as they are stronger acids than unsubstituted phenols. A global assessment of cloud chemistry involving aromatics oxidation products is possible with the modelling system used here (Tost et al., 2006, 2010). However, considering the complexity of aqueous-phase oxidation of organic compounds, such an assessment is outside the scope of this study and deserves a dedicated model study.

In our study, biomass burning emissions of aromatics are potentially underestimated. In fact, based on the recent update by Andreae (2019), we estimate that emissions might be up to 5 $\mathrm{Tg/yr}$ (65%) higher than what is implemented in our model. Moreover, emissions from peat fires in 2010 (the simulated year) were up to a factor 15 lower than in the subsequent years (van der Werf et al., 2017). In general, the inter-annual variability of biomass burning is large and difficult to capture in a study such as the present one.

Finally, atmospheric levels of benzene and toluene simulated by our model were shown to underestimate many observations by at least 20% (Cabrera-Perez et al., 2016). It is worth noting that in Cabrera-Perez et al. (2016) the total emissions of aromatics were even slightly higher (2.6 $\mathrm{TgC/yr}$) than in the *AROM* simulation. This underestimate could be explained by an overestimate of the chemical sink in the troposphere by reaction with hydroxyl radical. However, the annual global mean concentration of hydroxyl radicals is potentially 10% too high (Lelieveld et al., 2016), which cannot account for model concentration biases that are larger than 20%. Therefore, we surmise that the impact of aromatics on the trace gas composition may be larger than estimated in this study.

5 Summary

This study investigates the effects of several monocyclic aromatics on the tropospheric gas-phase composition by means of the chemistry-climate model EMAC. When aromatics are introduced into our model calculations, large changes are seen for glyoxal and methyl glyoxal. For other species, our results show a relatively small importance of aromatics on the global scale. This is consistent with recent results by Yan et al. (2019) who used a simpler chemistry mechanism in the GEOS-Chem model. However, different from that study, we found a negative impact on global ozone. Our results also indicate that by including aromatics chemistry, free tropospheric OH is reduced, especially in the northern hemisphere. On a regional scale, the concentrations of several species change significantly, with relatively largest impacts in East Asia where emissions are higher.

https://doi.org/10.5194/acp-2020-461
Preprint. Discussion started: 2 June 2020


Atmospheric Chemistry and Physics Discussions

Regions with high NO_x concentrations show increases of OH and O_3. However, since these increases are counteracted by decreases downwind, i.e., in remote areas where NO_x concentrations are much lower, the net effects on large scales are small. Of the nitrogen compounds, mainly NO_3 and HONO are affected by the aromatics chemistry.

We conclude that, although the impact of aromatics is relatively minor on the global scale, it is important on regional scales, notably in the anthropogenic source regions, and especially in those where NO_x emissions are strongest. Given the uncertainties in the oxidation mechanisms and emissions, the results of our model calculations may underestimate the impact of aromatics on the tropospheric gas-phase composition.

Code availability. The Modular Earth Submodel System (MESSy) is continuously further developed and applied by a consortium of institutions. The usage of MESSy and access to the source code is licensed to all affiliates of institutions which are members ofthe MESSy Consortium. Institutions can be a member of the MESSy Consortium by signing the MESSy Memorandum of Understanding. More information can be found on theMESSy Consortium web-page (http://www.messy-interface.org).

Author contributions. DT, RS, AP and DC wrote the manuscript. AP and DC performed the model simulations. DT and RS developed and analyzed the chemical mechanism. SB visualized the model results. SG performed extended budgeting of species' chemical turnover. All co-authors contributed to the analysis of results and the writing of the paper.

Competing interests. The authors have no competing interests

Acknowledgements. The authors want to acknowledge the use of the Ferret program for analysis and graphics in this paper. Ferret is a product of NOAA's Pacific Marine Environmental Laboratory (information is available at http://www.ferret.noaa.gov).

https://doi.org/10.5194/acp-2020-461
Preprint. Discussion started: 2 June 2020

Atmospheric Chemistry and Physics Discussions

Table 1. Global annual emission rates of aromatic compounds included in the model simulations and their relative contributions.

Species	total (TgC/a)	anthropogenic (EDGAR)	biomass burning (BIOBURN)	biogenic (MEGAN)
Benzene	4.417	70 %	30 %	
Toluene	5.888	82 %	13 %	5 %
Xylenes	5.664	96 %	4 %	
Ethylbenzene	1.961	74 %	26 %	
Benzaldehyde	1.382	92 %	6 %	2 %
Phenol	2.559	43 %	57 %	
Styrene	1.596	91 %	9 %	
Trimethylbenzenes	0.906	94 %	6 %	
Higher aromatics	4.980	48 %	52 %	

Table 2. Sensitivity studies.

Simulation	Description
AROM	Aromatics are fully included
NOAROM (reference)	No aromatics (emissions switched off)
ONLYMCM	Only MCM reactions

https://doi.org/10.5194/acp-2020-461
Preprint. Discussion started: 2 June 2020

Atmospheric Chemistry and Physics Discussions

Can you confirm that these are area weighted? The surface ozone seems a bit high compared to other models I've seen.

Table 3. Globally averaged mixing ratios at the surface (annual averages for 2010). "ABSDIFF" denotes the absolute difference, (e.g., AROM-NOAROM), and "RELDIFF" the relative difference, (e.g., AROM/NOAROM-1).

				AROM vs *ONLYMCM*		*AROM* vs *NOAROM*	
	NOAROM	*ONLYMCM*	*AROM*	ABSDIFF	RELDIFF	ABSDIFF	RELDIFF
	mol/mol	mol/mol	mol/mol	mol/mol	%	mol/mol	%
OH	4.630×10^{-14}	4.472×10^{-14}	4.487×10^{-14}	1.557×10^{-16}	0.3482	-1.425×10^{-15}	-3.078
O_3	3.269×10^{-8}	3.220×10^{-8}	3.190×10^{-8}	-2.964×10^{-10}	-0.9204	-7.888×10^{-10}	-2.413
NO	3.029×10^{-11}	2.793×10^{-11}	2.609×10^{-11}	-1.843×10^{-12}	-6.599	-4.203×10^{-12}	-13.87
NO_2	3.389×10^{-10}	3.314×10^{-10}	3.191×10^{-10}	-1.228×10^{-11}	-3.706	-1.977×10^{-11}	-5.834
NO_3	1.004×10^{-12}	9.462×10^{-13}	1.080×10^{-12}	1.339×10^{-13}	14.15	7.599×10^{-14}	7.568
HONO	7.393×10^{-12}	7.260×10^{-12}	7.315×10^{-12}	5.538×10^{-14}	0.7628	-7.754×10^{-14}	-1.049
HNO_3	1.420×10^{-10}	1.393×10^{-10}	1.426×10^{-10}	3.352×10^{-12}	2.407	6.607×10^{-13}	0.4653
HCHO	5.993×10^{-10}	5.992×10^{-10}	6.002×10^{-10}	9.484×10^{-13}	0.1583	8.414×10^{-13}	0.1404
glyoxal	1.040×10^{-11}	1.444×10^{-11}	1.505×10^{-11}	6.117×10^{-13}	4.237	4.646×10^{-12}	44.67
methyl glyoxal	3.847×10^{-11}	4.005×10^{-11}	4.015×10^{-11}	1.051×10^{-13}	0.2625	1.682×10^{-12}	4.372
benzaldehyde		6.798×10^{-12}	4.479×10^{-12}	-2.319×10^{-12}	-34.11	4.479×10^{-12}	
CO	97.6×10^{-9}	103.3×10^{-9}	103.3×10^{-9}	-6.5×10^{-11}	-0.06278	5.7×10^{-9}	5.847

Table 4. Simulated tropospheric integrals of OH, O_3 and NO_x, and the lifetime τ of CH_4.

	n(OH)		$m(O_3)$		$n(NO_x)$		$\tau(CH_4)$	
Simulation	NH	SH	NH	SH	NH	SH	NH	SH
NOAROM	6799 kmol	5765 kmol	207 Tg	173 Tg	7.90 Gmol	4.02 Gmol	7.36 yrs	9.61 yrs
ONLYMCM vs *NOAROM*	−9.9 %	−7.3 %	−2.5 %	−2.1 %	−3.7 %	−1.0 %	+7.1 %	+4.7 %
AROM vs *NOAROM*	−9 %	−6.3 %	−3.5 %	−2.3 %	−10.8 %	−4.5 %	+6.8 %	+4.5 %

https://doi.org/10.5194/acp-2020-461
Preprint. Discussion started: 2 June 2020

Atmospheric Chemistry and Physics Discussions

Table 5. Regionally averaged mixing ratios of selected species (annual averages for 2010).

	NOAROM mol/mol	*AROM* mol/mol	ABSDIFF mol/mol	RELDIFF %
		OH		
AMA	2.861×10^{-14}	2.785×10^{-14}	-7.689×10^{-16}	-2.687
CAF	6.447×10^{-14}	6.086×10^{-14}	-3.616×10^{-15}	-5.608
EAS	4.712×10^{-14}	5.527×10^{-14}	8.147×10^{-15}	17.29
EUR	3.591×10^{-14}	3.852×10^{-14}	2.615×10^{-15}	7.283
EUS	5.629×10^{-14}	5.784×10^{-14}	1.553×10^{-15}	2.759
		O_3		
AMA	2.979×10^{-8}	2.909×10^{-8}	-6.973×10^{-10}	-2.341
CAF	3.856×10^{-8}	3.712×10^{-8}	-1.440×10^{-9}	-3.733
EAS	3.124×10^{-8}	3.505×10^{-8}	3.807×10^{-9}	12.19
EUR	3.045×10^{-8}	3.033×10^{-8}	-1.250×10^{-10}	-0.4105
EUS	3.930×10^{-8}	3.904×10^{-8}	-2.604×10^{-10}	-0.6626
		NO_3		
AMA	3.570×10^{-13}	3.483×10^{-13}	-8.678×10^{-15}	-2.431
CAF	2.105×10^{-12}	2.321×10^{-12}	2.163×10^{-13}	10.27
EAS	1.833×10^{-12}	1.949×10^{-12}	1.163×10^{-13}	6.346
EUR	1.280×10^{-12}	1.256×10^{-12}	-2.448×10^{-14}	-1.913
EUS	2.536×10^{-12}	2.488×10^{-12}	-4.802×10^{-14}	-1.894
		HONO		
AMA	5.335×10^{-11}	5.349×10^{-11}	1.370×10^{-13}	0.2567
CAF	8.110×10^{-11}	8.227×10^{-11}	1.174×10^{-12}	1.447
EAS	1.152×10^{-10}	1.038×10^{-10}	-1.146×10^{-11}	-9.945
EUR	5.689×10^{-11}	5.604×10^{-11}	-8.429×10^{-13}	-1.482
EUS	4.415×10^{-11}	4.230×10^{-11}	-1.854×10^{-12}	-4.199
		HNO_3		
AMA	1.515×10^{-10}	1.508×10^{-10}	-7.056×10^{-13}	-0.4657
CAF	4.957×10^{-10}	5.162×10^{-10}	2.048×10^{-11}	4.131
EAS	1.035×10^{-9}	1.169×10^{-9}	1.335×10^{-10}	12.89
EUR	3.985×10^{-10}	4.003×10^{-10}	1.855×10^{-12}	0.4656
EUS	6.706×10^{-10}	6.721×10^{-10}	1.505×10^{-12}	0.2244
		HCHO		
AMA	5.217×10^{-9}	5.189×10^{-9}	-2.874×10^{-11}	-0.5509
CAF	3.468×10^{-9}	3.478×10^{-9}	9.392×10^{-12}	0.2708
EAS	1.322×10^{-9}	1.557×10^{-9}	2.348×10^{-10}	17.76
EUR	7.356×10^{-10}	7.708×10^{-10}	3.517×10^{-11}	4.781
EUS	1.911×10^{-9}	1.942×10^{-9}	3.096×10^{-11}	1.620

https://doi.org/10.5194/acp-2020-461
Preprint. Discussion started: 2 June 2020

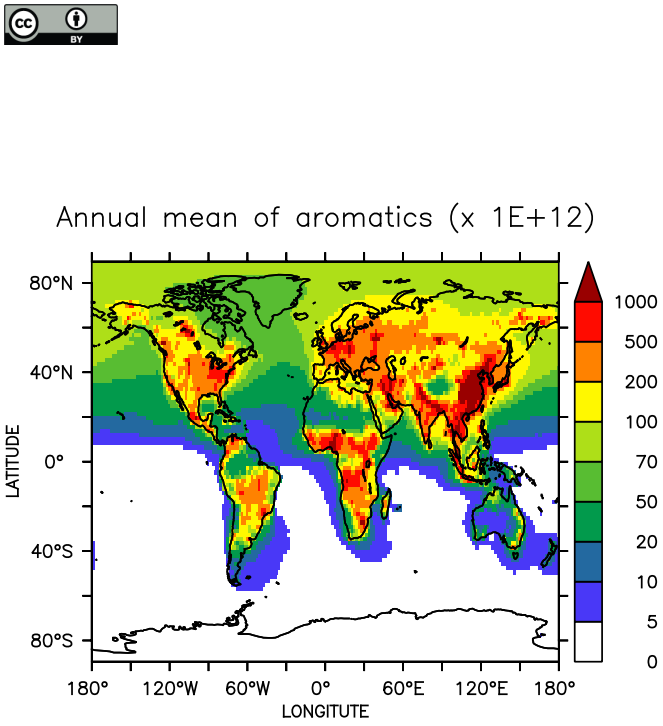

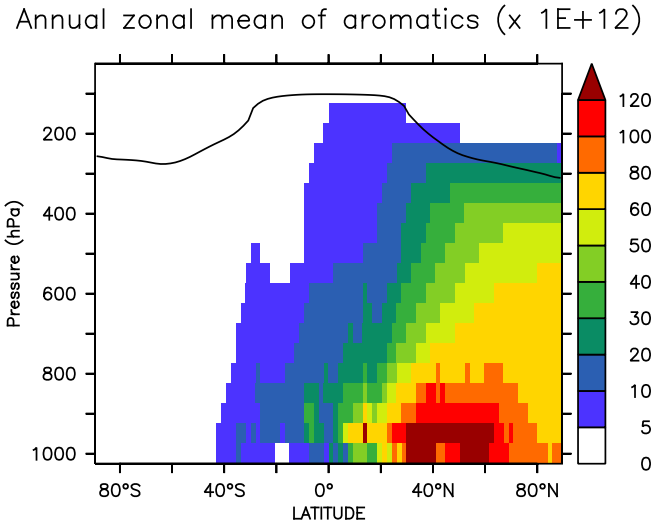

Figure 1. Annual mean mixing ratios of the sum of aromatics at the surface (left) and the zonal mean (right) in the *AROM* simulation. The solid line between 100 and 300 hPa depicts the mean tropopause level.

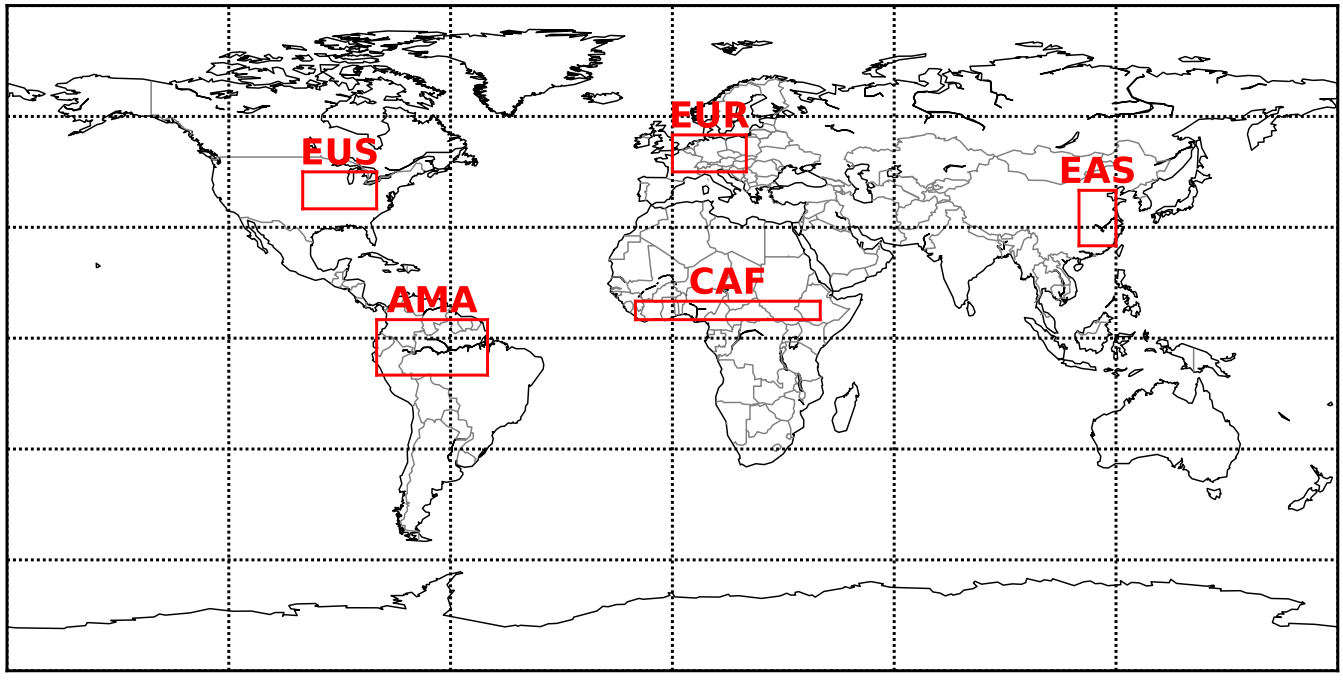

Figure 2. Selected regions: AMA = Amazon area, CAF = central Africa, EAS = eastern Asia, EUR = Europe, EUS = eastern US.

https://doi.org/10.5194/acp-2020-461
Preprint. Discussion started: 2 June 2020

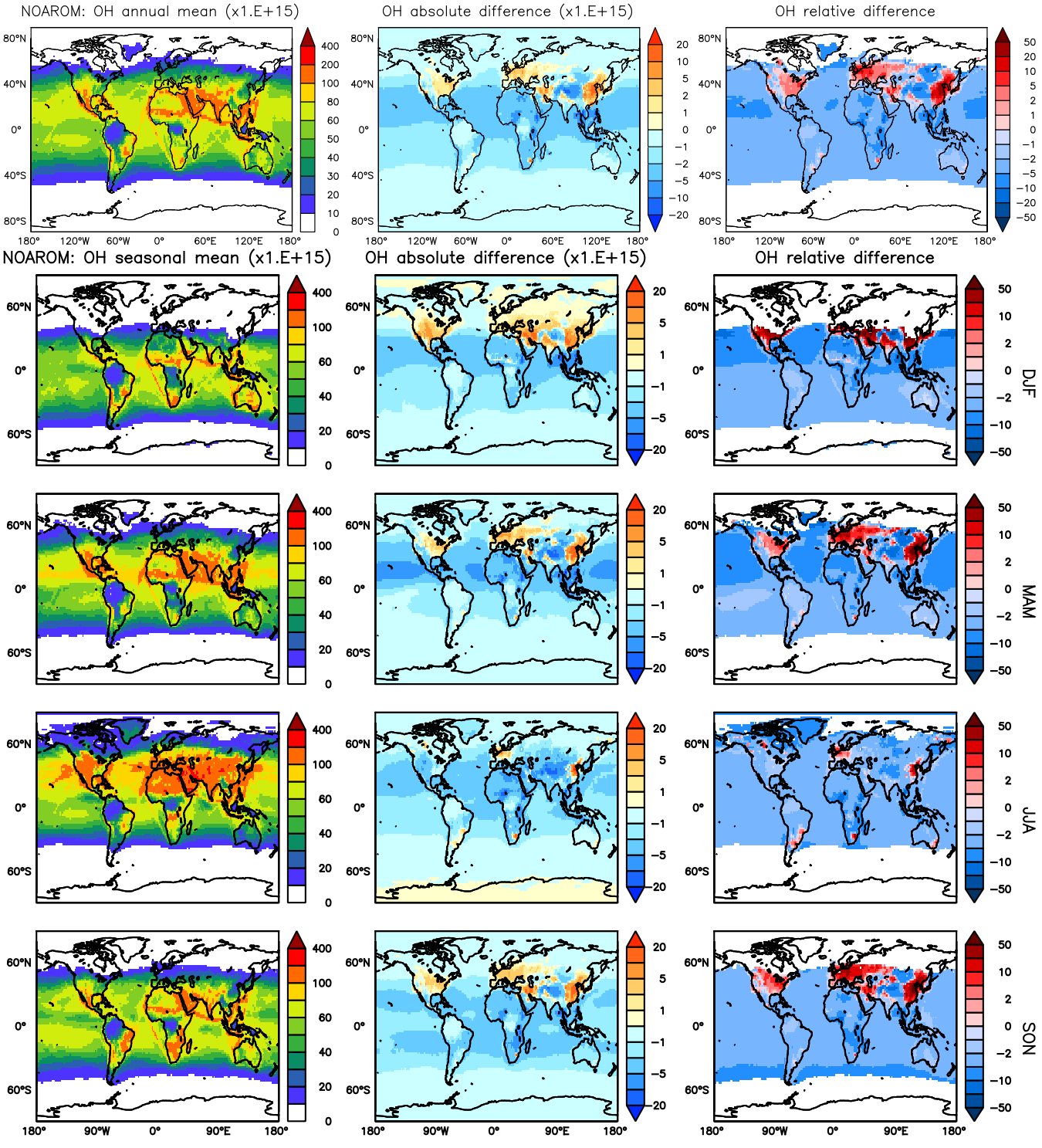

Figure 3. Annual average OH mixing ratios at the surface. Middle rows: Seasonal means. Left column: Mixing ratios in the *NOAROM* simulation. Middle column: Absolute difference *AROM-NOAROM*. Right column: Relative difference *AROM*/*NOAROM*-1 in % (shown only where OH is above 0.01 pmol/mol).

https://doi.org/10.5194/acp-2020-461
Preprint. Discussion started: 2 June 2020

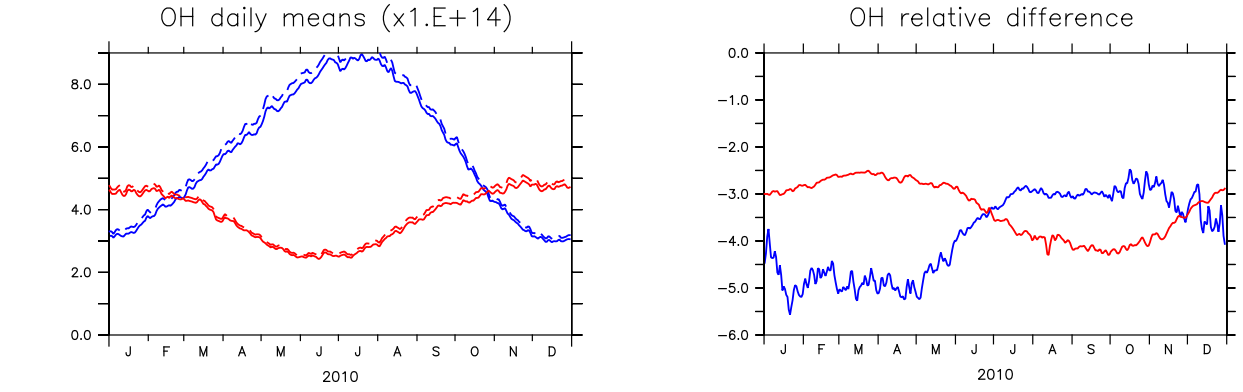

Figure 4. Seasonal cycle of OH daily (24 h) mixing ratio means in the planetary boundary layer (PBL) and relative difference (expressed in %) between *AROM* (solid) and *NOAROM* (dashed). In blue, values for the NH; in red, values for the SH. The PBL diagnosis is described in Pozzer et al. (2009). The PBL is calculated in the model based on the work of Holtslag et al. (1990). An interactive calculation is performed following the approach of Troen and Mahrt (1986), using the Richardson number, the horizontal velocity components, the buoyancy parameters and the virtual temperature (Holtslag and Boville, 1993).

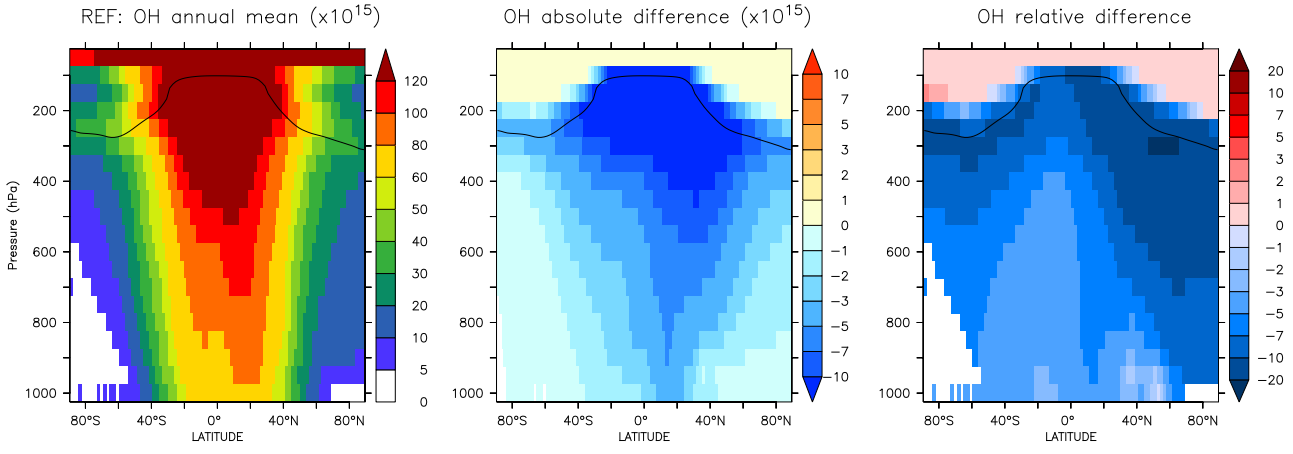

Figure 5. Annual average zonal mean OH mixing ratios. Left: Mixing ratios in the *NOAROM* simulation. Middle: Absolute difference *AROM*-*NOAROM*. Right: Relative difference *AROM*/*NOAROM*-1 in %. The solid line between 100 and 300 hPa depicts the mean tropopause level.

https://doi.org/10.5194/acp-2020-461
Preprint. Discussion started: 2 June 2020

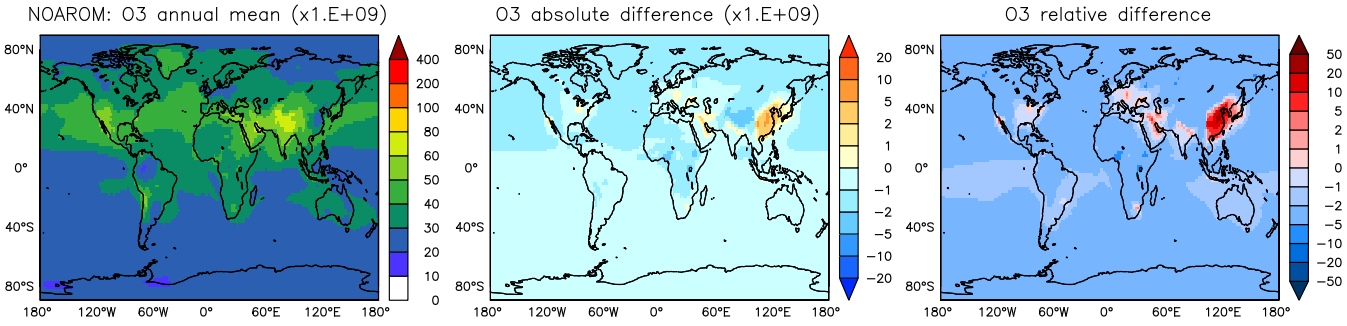

Figure 6. Annual average O_3 mixing ratios at the surface. Left: Mixing ratios in the *NOAROM* simulation. Middle: Absolute difference *AROM-NOAROM*. Right: Relative difference *AROM*/*NOAROM*-1 in %.

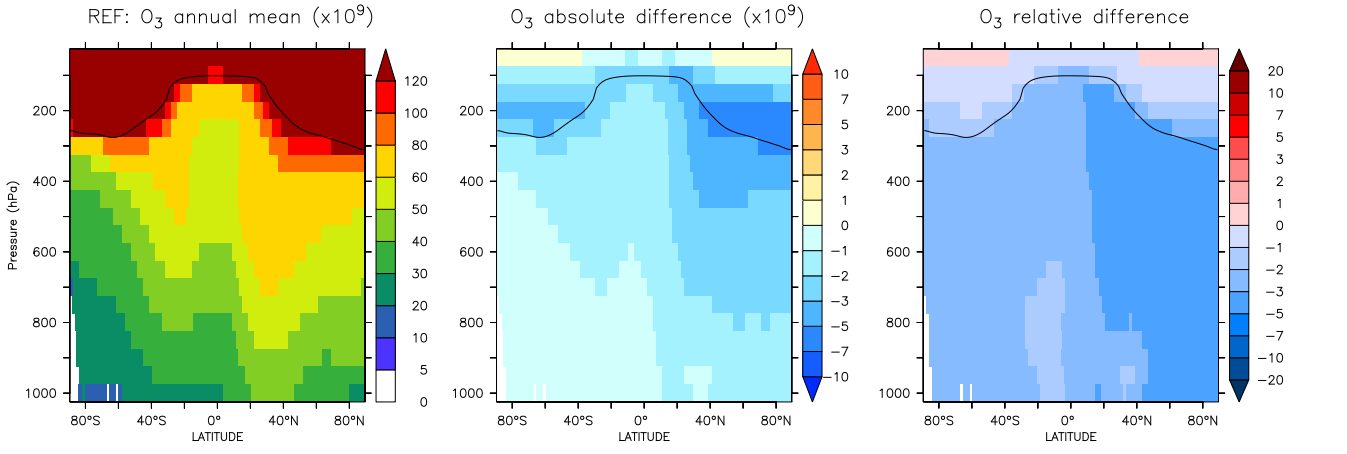

Figure 7. Annual average zonal mean O_3 mixing ratios. Left: Mixing ratios in the *NOAROM* simulation. Middle: Absolute difference *AROM-NOAROM*. Right: Relative difference *AROM*/*NOAROM*-1 in %. The solid line between 100 and 300 hPa depicts the mean tropopause level.

https://doi.org/10.5194/acp-2020-461
Preprint. Discussion started: 2 June 2020

Atmospheric Chemistry and Physics Discussions

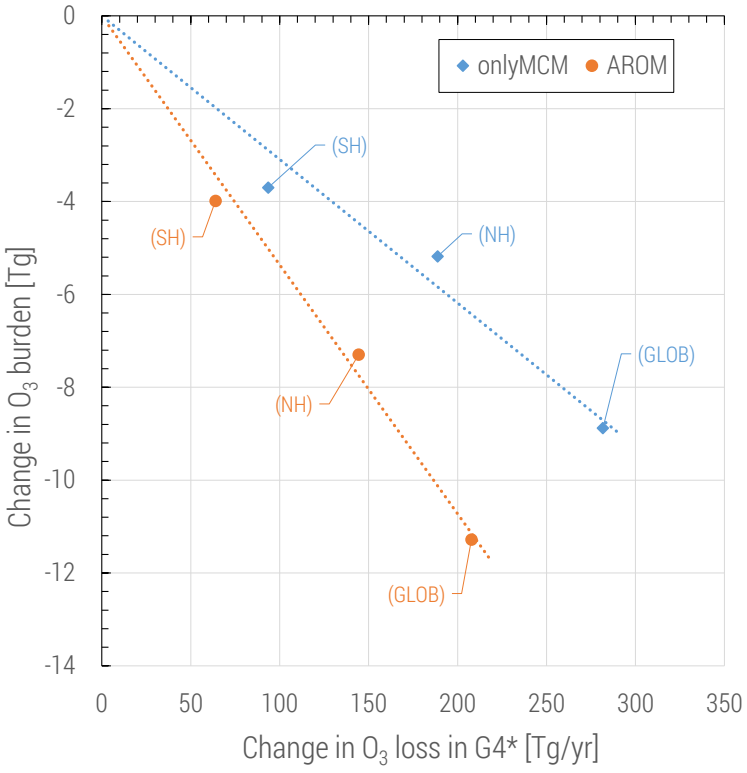

Figure 8. Change in tropospheric ozone burden versus change in ozone loss for all reactions in the VOC chemistry (G4 category of the MECCA mechanism[, see the Supplement of (Sander et al., 2019)]). The change in ozone loss is due to the reactions with (substituted) phenoxy radicals. Global and hemispheric results for *onlyMCM* (blue) and *AROM* (orange) simulations are shown.

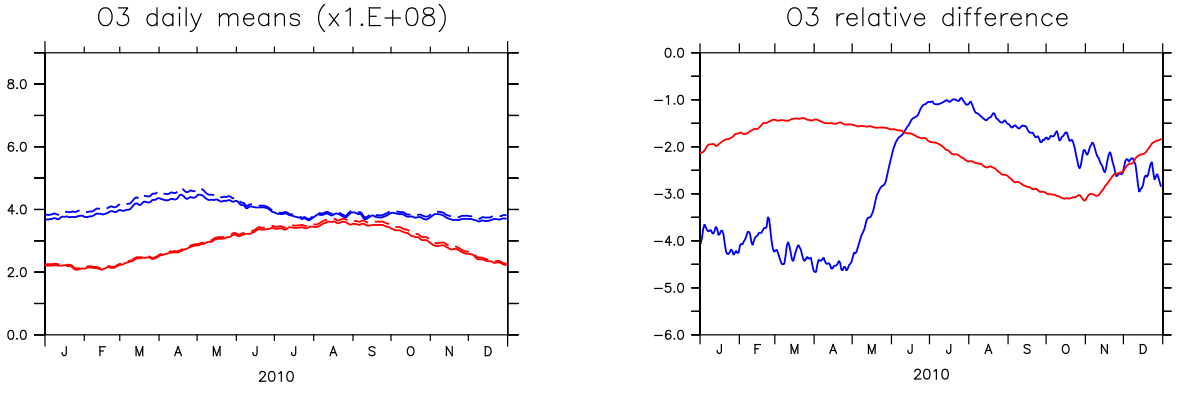

Figure 9. Same as in Fig. 4 for ozone.

https://doi.org/10.5194/acp-2020-461
Preprint. Discussion started: 2 June 2020

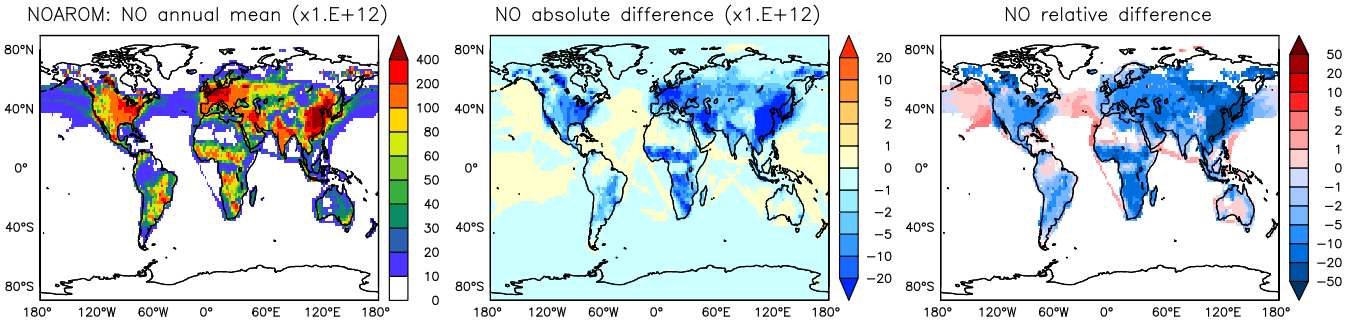

Figure 10. Annual average NO mixing ratios at the surface. Left: Mixing ratios in the *NOAROM* simulation. Middle: Absolute difference *AROM-NOAROM*. Right: Relative difference *AROM*/*NOAROM*-1 in % (shown only where NO is above 10 pmol/mol).

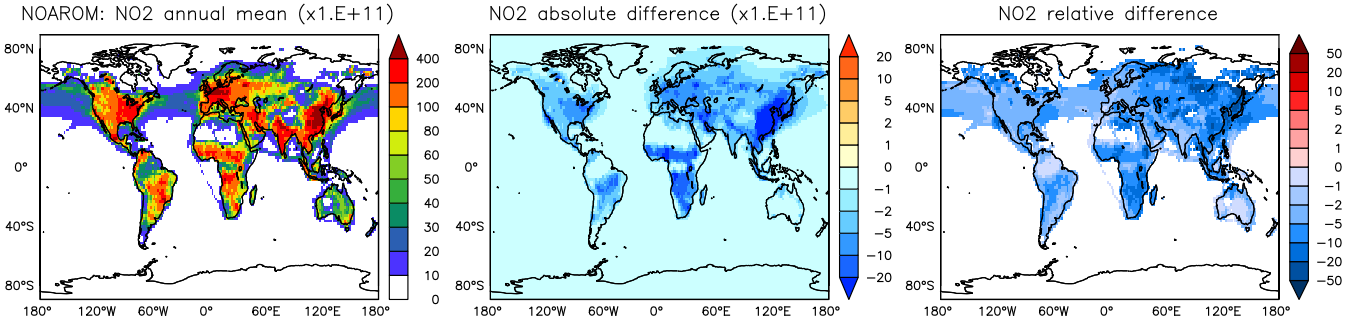

Figure 11. Annual average NO_2 mixing ratios at the surface. Left: Mixing ratios in the *NOAROM* simulation. Middle: Absolute difference *AROM-NOAROM*. Right: Relative difference *AROM*/*NOAROM*-1 in % (shown only where NO_2 is above 100 pmol/mol).

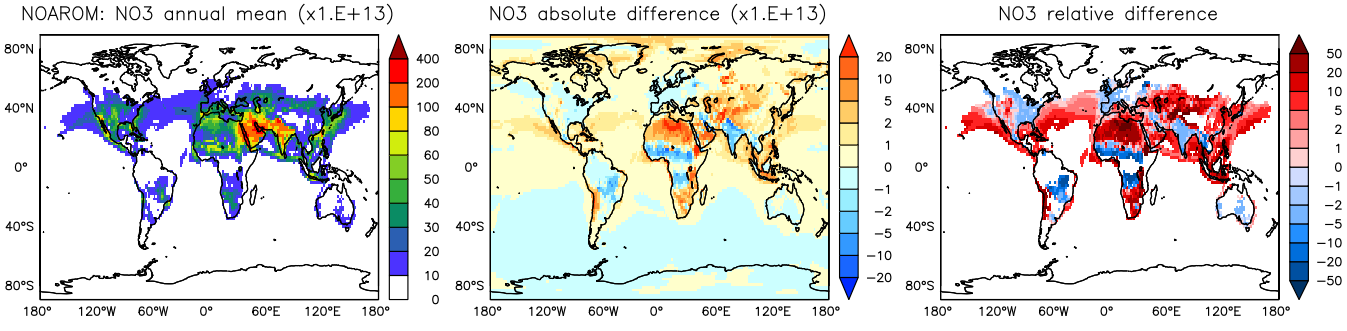

Figure 12. Annual average NO_3 mixing ratios at the surface. Left: Mixing ratios in the *NOAROM* simulation. Middle: Absolute difference *AROM-NOAROM*. Right: Relative difference *AROM*/*NOAROM*-1 in % (shown only where NO_3 is above 1 pmol/mol).

https://doi.org/10.5194/acp-2020-461
Preprint. Discussion started: 2 June 2020

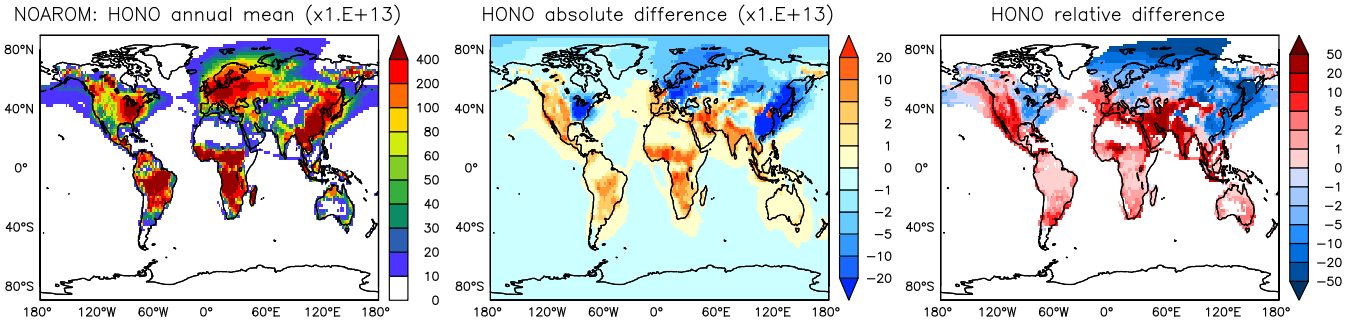

Figure 13. Annual average HONO mixing ratios at the surface. Left: Mixing ratios in the *NOAROM* simulation. Middle: Absolute difference *AROM-NOAROM*. Right: Relative difference *AROM*/*NOAROM*-1 in % (shown only where HONO is above 1 pmol/mol).

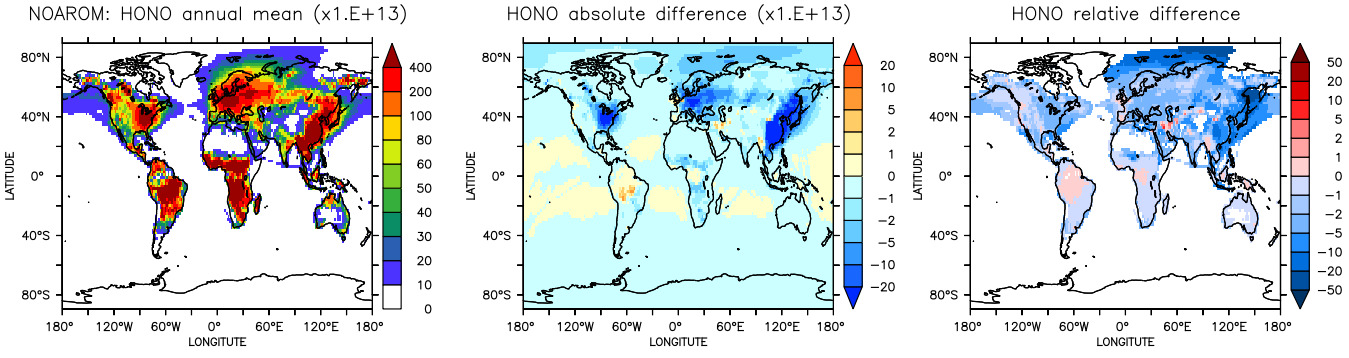

Figure 14. Annual average HONO mixing ratios at the surface. Left: Mixing ratios in the *NOAROM* simulation. Middle: Absolute difference *ONLYMCM-NOAROM*. Right: Relative difference *ONLYMCM*/*NOAROM*-1 in % (shown only where HONO is above 1 pmol/mol).

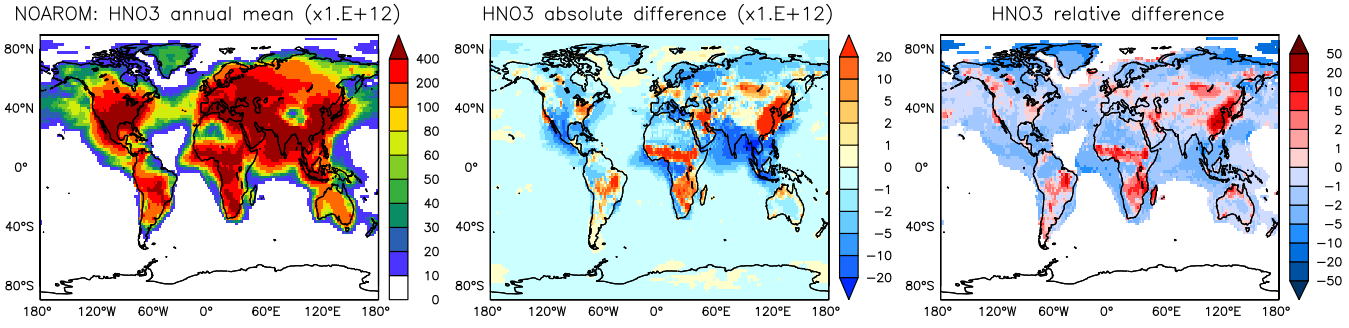

Figure 15. Annual average HNO_3 mixing ratios at the surface. Left: Mixing ratios in the *NOAROM* simulation. Middle: Absolute difference *AROM-NOAROM*. Right: Relative difference *AROM*/*NOAROM*-1 in % (shown only where HNO_3 is above 10 pmol/mol).

https://doi.org/10.5194/acp-2020-461
Preprint. Discussion started: 2 June 2020

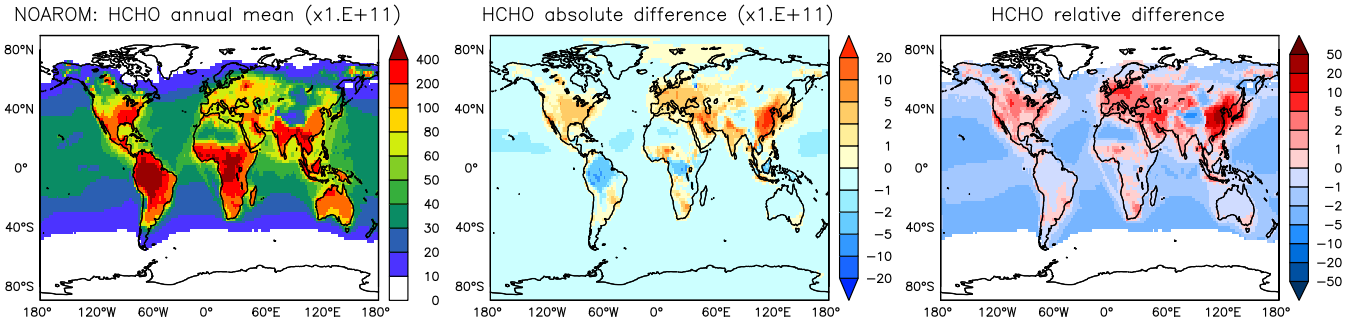

Figure 16. Annual average HCHO mixing ratios at the surface. Left: Mixing ratios in the *NOAROM* simulation. Middle: Absolute difference *AROM-NOAROM*. Right: Relative difference *AROM*/*NOAROM*-1 in % (shown only where HCHO is above 100 pmol/mol).

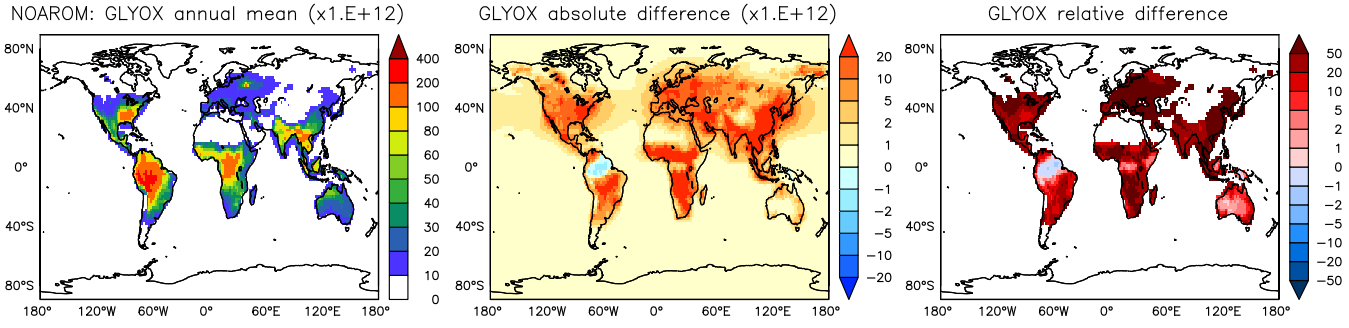

Figure 17. Annual average glyoxal mixing ratios at the surface. Left: Mixing ratios in the *NOAROM* simulation. Middle: Absolute difference *AROM-NOAROM*. Right: Relative difference *AROM*/*NOAROM*-1 in % (shown only where glyoxal is above 10 pmol/mol).

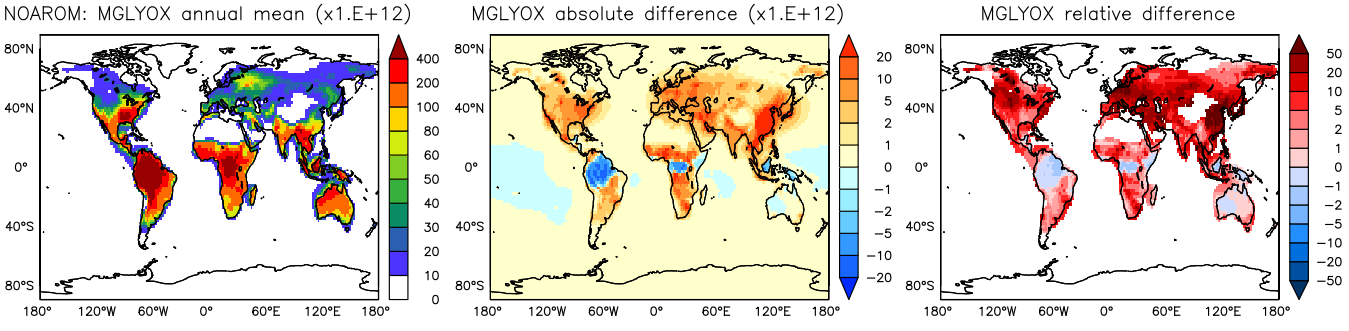

Figure 18. Annual average methyl glyoxal mixing ratios at the surface. Left: Mixing ratios in the *NOAROM* simulation. Middle: Absolute difference *AROM-NOAROM*. Right: Relative difference *AROM*/*NOAROM*-1 in % (shown only where methyl glyoxal is above 10 pmol/mol).

https://doi.org/10.5194/acp-2020-461
Preprint. Discussion started: 2 June 2020

Atmospheric Chemistry and Physics Discussions

References

Andreae, M. O.: Emission of trace gases and aerosols from biomass burning – an updated assessment, Atmospheric Chemistry and Physics, 19, 8523–8546, https://doi.org/10.5194/acp-19-8523-2019, https://www.atmos-chem-phys.net/19/8523/2019/, 2019.

Atkinson, R., Aschmann, S. M., Arey, J., and Carter, W. P.: Formation of ring-retaining products from the OH radical-initiated reactions of benzene and toluene, Int. J. Chem. Kinetics, 21, 801–827, 1989.

Barletta, B., Meinardi, S., Sherwood Rowland, F., Chan, C.-Y., Wang, X., Zou, S., Yin Chan, L., and Blake, D. R.: Volatile organic compounds in 43 Chinese cities, Atmos. Environ., 39, 5979–5990, 2005.

Bejan, I., El Aal, Y. A., Barnes, I., Benter, T., Bohn, B., Wiesen, P., and Kleffmann, J.: The photolysis of ortho-nitrophenols: a new gas phase source of HONO, Phys. Chem. Chem. Phys., 8, 2028–2035, 2006.

Birdsall, A. W., Andreoni, J. F., and Elrod, M. J.: Investigation of the role of bicyclic peroxy radicals in the oxidation mechanism of toluene, J. Phys. Chem. A, 114, 10 655–10 663, https://doi.org/10.1021/jp105467e, 2010.

Bloss, C., Wagner, V., Bonzanini, A., Jenkin, M. E., Wirtz, K., Martin-Reviejo, M., and Pilling, M. J.: Evaluation of detailed aromatic mechanisms (MCMv3 and MCMv3.1) against environmental chamber data, Atmos. Chem. Phys., 5, 623–639, https://doi.org/10.5194/acp-5-623-2005, https://www.atmos-chem-phys.net/5/623/2005/, 2005a.

Bloss, C., Wagner, V., Jenkin, M. E., Volkamer, R., Bloss, W. J., Lee, J. D., Heard, D. E., Wirtz, K., Martin-Reviejo, M., Rea, G., Wenger, J. C., and Pilling, M. J.: Development of a detailed chemical mechanism (MCMv3.1) for the atmospheric oxidation of aromatic hydrocarbons, Atmos. Chem. Phys., 5, 641–664, https://doi.org/10.5194/acp-5-641-2005, 2005b.

Cabrera-Perez, D., Taraborrelli, D., Sander, R., and Pozzer, A.: Global atmospheric budget of simple monocyclic aromatic compounds, Atmos. Chem. Phys., 16, 6931–6947, https://doi.org/10.5194/acp-16-6931-2016, 2016.

Carter, W. P. and Heo, G.: Development of revised SAPRC aromatics mechanisms, Atmospheric Environment, 77, 404 – 414, https://doi.org/https://doi.org/10.1016/j.atmosenv.2013.05.021, http://www.sciencedirect.com/science/article/pii/S1352231013003646, 2013.

Cheng, S.-B., Zhou, C.-H., Yin, H.-M., Sun, J.-L., and Han, K.-L.: OH produced from o-nitrophenol photolysis: a combined experimental and theoretical investigation, J. Chem. Phys., 130, 234 311–234 311, 2009.

Daniel, J. S. and Solomon, S.: On the climate forcing of carbon monoxide, J. Geophys. Res., 103, 13 249–13 260, 1998.

Deckert, R., Jöckel, P., Grewe, V., Gottschaldt, K.-D., and Hoor, P.: A quasi chemistry-transport model mode for EMAC, Geosci. Model Dev., 4, 195–206, 2011.

Emmons, L. K., Walters, S., Hess, P. G., Lamarque, J.-F., Pfister, G. G., Fillmore, D., Granier, C., Guenther, A., Kinnison, D., Laepple, T., Orlando, J., Tie, X., Tyndall, G., Wiedinmyer, C., Baughcum, S. L., and Kloster, S.: Description and evaluation of the Model for Ozone and Related chemical Tracers, version 4 (MOZART-4), Geosci. Model Dev., 3, 43–67, https://doi.org/10.5194/gmd-3-43-2010, 2010.

Epstein, S. A., Riipinen, I., and Donahue, N. M.: A semiempirical correlation between enthalpy of vaporization and saturation concentration for organic aerosol, Environ. Sci. Technol., 44, 743–748, https://doi.org/10.1021/es902497z, 2010.

Field, R. J., Raghavan, N. V., and Brummer, J. G.: A pulse radiolysis investigation of the reactions of bromine dioxide radical (BrO2.cntdot.) with hexacyanoferrate(II), manganese(II), phenoxide ion, and phenol, The Journal of Physical Chemistry, 86, 2443–2449, https://doi.org/10.1021/j100210a040, https://doi.org/10.1021/j100210a040, 1982.

https://doi.org/10.5194/acp-2020-461
Preprint. Discussion started: 2 June 2020

Atmospheric Chemistry and Physics Discussions

Guenther, A. B., Jiang, X., Heald, C. L., Sakulyanontvittaya, T., Duhl, T., Emmons, L. K., and Wang, X.: The Model of Emissions of Gases and Aerosols from Nature version 2.1 (MEGAN2.1): an extended and updated framework for modeling biogenic emissions, Geosci. Model Dev., 5, 1471–1492, https://doi.org/10.5194/gmd-5-1471-2012, 2012.

Hoigné, J. and Bader, H.: Rate constants of reactions of ozone with organic and inorganic compounds in water—II: Dissociating organic compounds, Water Research, 17, 185 – 194, https://doi.org/https://doi.org/10.1016/0043-1354(83)90099-4, http://www.sciencedirect.com/science/article/pii/0043135483900994, 1983.

Holtslag, A. and Boville, B.: Local versus nonlocal boundary-layer diffusion in a global climate model, J. Clim., 6, 1825–1842, 1993.

Holtslag, A., De Bruijn, E., and Pan, H.: A high resolution air mass transformation model for short-range weather forecasting, Monthly Weather Review, 118, 1561–1575, 1990.

Hu, L., Millet, D. B., Baasandorj, M., Griffis, T. J., Travis, K. R., Tessum, C. W., Marshall, J. D., Reinhart, W. F., Mikoviny, T., Müller, M., Wisthaler, A., Graus, M., Warneke, C., and de Gouw, J.: Emissions of C_6–C_8 aromatic compounds in the United States: Constraints from tall tower and aircraft measurements, J. Geophys. Res., 120, https://doi.org/10.1002/2014JD022627, 2015.

Huang, G., Brook, R., Crippa, M., Janssens-Maenhout, G., Schieberle, C., Dore, C., Guizzardi, D., Muntean, M., Schaaf, E., and Friedrich, R.: Speciation of anthropogenic emissions of non-methane volatile organic compounds: a global gridded data set for 1970–2012, Atmos. Chem. Phys., 17, 7683–7701, https://doi.org/10.5194/acp-17-7683-2017, 2017.

Jagiella, S. and Zabel, F.: Reaction of phenylperoxy radicals with NO_2 at 298 K, Phys. Chem. Chem. Phys., 9, 5036–5051, https://doi.org/10.1039/B705193J, 2007.

Jenkin, M. E., Saunders, S. M., Wagner, V., and Pilling, M. J.: Protocol for the development of the Master Chemical Mechanism, MCM v3 (part B): tropospheric degradation of aromatic volatile organic compounds, Atmos. Chem. Phys., 3, 181–193, https://doi.org/10.5194/acp-3-181-2003, 2003.

Jöckel, P., Kerkweg, A., Pozzer, A., Sander, R., Tost, H., Riede, H., Baumgaertner, A., Gromov, S., and Kern, B.: Development cycle 2 of the Modular Earth Submodel System (MESSy2), Geosci. Model Dev., 3, 717–752, https://doi.org/10.5194/GMD-3-717-2010, 2010.

Jöckel, P., Tost, H., Pozzer, A., Kunze, M., Kirner, O., Brenninkmeijer, C. A. M., Brinkop, S., Cai, D. S., Dyroff, C., Eckstein, J., Frank, F., Garny, H., Gottschaldt, K.-D., Graf, P., Grewe, V., Kerkweg, A., Kern, B., Matthes, S., Mertens, M., Meul, S., Neumaier, M., Nützel, M., Oberländer-Hayn, S., Ruhnke, R., Runde, T., Sander, R., Scharffe, D., and Zahn, A.: Earth System Chemistry integrated Modelling (ESCiMo) with the Modular Earth Submodel System (MESSy), version 2.51, Geosci. Model Dev., 9, 1153–1200, https://doi.org/10.5194/gmd-9-1153-2016, 2016.

Kaiser, J. W., Heil, A., Andreae, M. O., Benedetti, A., Chubarova, N., Jones, L., Morcrette, J.-J., Razinger, M., Schultz, M. G., Suttie, M., and van der Werf, G. R.: Biomass burning emissions estimated with a global fire assimilation system based on observed fire radiative power, Biogeosci., 9, 527–554, https://doi.org/10.5194/bg-9-527-2012, 2012.

Koppmann, R.: Volatile organic compounds in the atmosphere, Blackwell Publishing Ltd, https://doi.org/10.1002/9780470988657, 2007.

Lee, S., Chiu, M., Ho, K., Zou, S., and Wang, X.: Volatile organic compounds (VOCs) in urban atmosphere of Hong Kong, Chemosphere, 48, 375–382, 2002.

Lelieveld, J. and Crutzen, P. J.: Influences of cloud photochemical processes on tropospheric ozone, Nature, 343, 227–233, https://doi.org/10.1038/343227A0, 1990.

Lelieveld, J., Gromov, S., Pozzer, A., and Taraborrelli, D.: Global tropospheric hydroxyl distribution, budget and reactivity, Atmos. Chem. Phys., 16, 12 477–12 493, https://doi.org/10.5194/acp-16-12477-2016, 2016.

https://doi.org/10.5194/acp-2020-461
Preprint. Discussion started: 2 June 2020

Atmospheric Chemistry and Physics Discussions

Li, Y., Pöschl, U., and Shiraiwa, M.: Molecular corridors and parameterizations of volatility in the chemical evolution of organic aerosols, Atmos. Chem. Phys., 16, 3327–3344, https://doi.org/10.5194/acp-16-3327-2016, 2016.

Lin, G., Penner, J. E., Sillman, S., Taraborrelli, D., and Lelieveld, J.: Global modeling of SOA formation from dicarbonyls, epoxides, organic nitrates and peroxides, Atmos. Chem. Phys., 12, 4743–4774, https://doi.org/10.5194/acp-12-4743-2012, 2012.

Misztal, P., Hewitt, C., Wildt, J., Blande, J., Eller, A., Fares, S., Gentner, D., Gilman, J., Graus, M., Greenberg, J., Guenther, A., Hansel, A., Harley, P., Huang, M., Jardine, K., Karl, T., Kaser, L., Keutsch, F., Kiendler-Scharr, A., Kleist, E., Lerner, B., Li, T., Mak, J., Nölscher, A., Schnitzhofer, R., Sinha, V., Thornton, B., Warneke, C., Wegener, F., Werner, C., Williams, J., Worton, D., Yassaa, N., and Goldstein, A.: Atmospheric benzenoid emissions from plants rival those from fossil fuels, Scientific Reports, 5, https://doi.org/10.1038/srep12064, 2015.

Ng, N. L., Kroll, J. H., Chan, A. W. H., Chhabra, P. S., Flagan, R. C., and Seinfeld, J. H.: Secondary organic aerosol formation from m-xylene, toluene, and benzene, Atmos. Chem. Phys., 7, 3909–3922, https://doi.org/10.5194/acp-7-3909-2007, 2007.

Pozzer, A., Jöckel, P., Tost, H., Sander, R., Ganzeveld, L., Kerkweg, A., and Lelieveld, J.: Simulating organic species with the global atmospheric chemistry general circulation model ECHAM5/MESSy1: a comparison of model results with observations, Atmos. Chem. Phys., 7, 2527–2550, https://doi.org/10.5194/ACP-7-2527-2007, 2007.

Pozzer, A., Jöckel, P., and van Aardenne, J.: The influence of the vertical distribution of emissions on tropospheric chemistry, Atmos. Chem. Phys., 9, 9417–9432, https://doi.org/10.5194/ACP-9-9417-2009, 2009.

Pozzer, A., Pollmann, J., Taraborrelli, D., Jöckel, P., Helmig, D., Tans, P., Hueber, J., and Lelieveld, J.: Observed and simulated global distribution and budget of atmospheric C_2-C_5 alkanes, Atmos. Chem. Phys., 10, 4403–4422, https://doi.org/10.5194/ACP-10-4403-2010, 2010.

Pringle, K. J., Tost, H., Message, S., Steil, B., Giannadaki, D., Nenes, A., Fountoukis, C., Stier, P., Vignati, E., and Lelieveld, J.: Description and evaluation of GMXe: a new aerosol submodel for global simulations (v1), Geosci. Model Dev., 3, 391–412, https://doi.org/10.5194/gmd-3-391-2010, 2010.

Ran, L., Zhao, C., Geng, F., Tie, X., Tang, X., Peng, L., Zhou, G., Yu, Q., Xu, J., and Guenther, A.: Ozone photochemical production in urban Shanghai, China: Analysis based on ground level observations, J. Geophys. Res., 114D, 2009.

Roeckner, E., Brokopf, R., Esch, M., Giorgetta, M., Hagemann, S., Kornblueh, L., Manzini, E., Schlese, U., and Schulzweida, U.: Sensitivity of simulated climate to horizontal and vertical resolution in the ECHAM5 atmosphere model, J. Clim., 19, 3771–3791, https://doi.org/10.1175/JCLI3824.1, 2006.

Roth, E., Chakir, A., and Ferhati, A.: Study of a benzoylperoxy radical in the gas phase: ultraviolet spectrum and $C_6H_5C(O)O_2$ + HO_2 reaction between 295 and 357 K, J. Phys. Chem. A, 114, 10 367–10 379, https://doi.org/10.1021/jp1021467, 2010.

Sack, T. M., Steele, D. H., Hammerstrom, K., and Remmers, J.: A survey of household products for volatile organic compounds, Atmos. Environ., 26A, 1063–1070, 1992.

Sander, R., Baumgaertner, A., Cabrera-Perez, D., Frank, F., Gromov, S., Grooß, J.-U., Harder, H., Huijnen, V., Jöckel, P., Karydis, V. A., Niemeyer, K. E., Pozzer, A., Riede, H., Schultz, M. G., Taraborrelli, D., and Tauer, S.: The community atmospheric chemistry box model CAABA/MECCA-4.0, Geosci. Model Dev., 12, 1365–1385, https://doi.org/10.5194/gmd-12-1365-2019, 2019.

Sherwen, T., Schmidt, J. A., Evans, M. J., Carpenter, L. J., Großmann, K., Eastham, S. D., Jacob, D. J., Dix, B., Koenig, T. K., Sinreich, R., Ortega, I., Volkamer, R., Saiz-Lopez, A., Prados-Roman, C., Mahajan, A. S., and Ordóñez, C.: Global impacts of tropospheric halogens (Cl, Br, I) on oxidants and composition in GEOS-Chem, Atmospheric Chemistry and Physics, 16, 12 239–12 271, https://doi.org/10.5194/acp-16-12239-2016, https://www.atmos-chem-phys.net/16/12239/2016/, 2016.

https://doi.org/10.5194/acp-2020-461
Preprint. Discussion started: 2 June 2020

Atmospheric Chemistry and Physics Discussions

Sillman, S., Logan, J. A., and Wofsy, S. C.: The sensitivity of ozone to nitrogen oxides and hydrocarbons in regional ozone episodes, J. Geophys. Res., 95D, 1837–1851, https://doi.org/10.1029/JD095iD02p01837, 1990.

Tao, Z. and Li, Z.: A kinetics study on reactions of C_6H_5O with C_6H_5O and O_3 at 298 K, Int. J. Chem. Kinet., 31, 65–72, https://doi.org/10.1002/(SICI)1097-4601(1999)31:1<65::AID-KIN8>3.0.CO;2-J, 1999.

Tilmes, S., Lamarque, J.-F., Emmons, L. K., Kinnison, D. E., Marsh, D., Garcia, R. R., Smith, A. K., Neely, R. R., Conley, A., Vitt, F., Val Martin, M., Tanimoto, H., Simpson, I., Blake, D. R., and Blake, N.: Representation of the Community Earth System Model (CESM1) CAM4-chem within the Chemistry-Climate Model Initiative (CCMI), Geoscientific Model Development, 9, 1853–1890, https://doi.org/10.5194/gmd-9-1853-2016, https://www.geosci-model-dev.net/9/1853/2016/, 2016.

Tost, H., Jöckel, P., Kerkweg, A., Sander, R., and Lelieveld, J.: Technical note: A new comprehensive SCAVenging submodel for global atmospheric chemistry modelling, Atmos. Chem. Phys., 6, 565–574, https://doi.org/10.5194/ACP-6-565-2006, 2006.

Tost, H., Lawrence, M. G., Brühl, C., Jöckel, P., The GABRIEL Team, and The SCOUT-O3-DARWIN/ACTIVE Team: Uncertainties in atmospheric chemistry modelling due to convection parameterisations and subsequent scavenging, Atmos. Chem. Phys., 10, 1931–1951, https://doi.org/10.5194/ACP-10-1931-2010, 2010.

Troen, I. and Mahrt, L.: A simple model of the atmospheric boundary layer; sensitivity to surface evaporation, Boundary-Layer Meteorology, 37, 129–148, 1986.

Tsimpidi, A. P., Karydis, V. A., Pozzer, A., Pandis, S. N., and Lelieveld, J.: ORACLE (v1.0): module to simulate the organic aerosol composition and evolution in the atmosphere, Geosci. Model Dev., 7, 3153–3172, https://doi.org/10.5194/gmd-7-3153-2014, 2014.

Tyndall, G. S., Wallington, T. J., and Ball, J. C.: FTIR Product Study of the Reactions CH3O2 + CH3O2 and CH3O2 + O3, The Journal of Physical Chemistry A, 102, 2547–2554, https://doi.org/10.1021/jp972784h, https://doi.org/10.1021/jp972784h, 1998.

van der Werf, G. R., Randerson, J. T., Giglio, L., van Leeuwen, T. T., Chen, Y., Rogers, B. M., Mu, M., van Marle, M. J. E., Morton, D. C., Collatz, G. J., Yokelson, R. J., and Kasibhatla, P. S.: Global fire emissions estimates during 1997–2016, Earth System Science Data, 9, 697–720, https://doi.org/10.5194/essd-9-697-2017, https://www.earth-syst-sci-data.net/9/697/2017/, 2017.

Vereecken, L.: Reaction Mechanisms for the Atmospheric Oxidation of Monocyclic Aromatic Compounds, chap. Chapter 6, pp. 377–527, World Scientific Publishing, https://doi.org/10.1142/9789813271838_0006, https://www.worldscientific.com/doi/abs/10.1142/9789813271838_0006, 2019.

Vereecken, L., Chakravarty, H. K., Bohn, B., and Lelieveld, J.: Theoretical Study on the Formation of H- and O-Atoms, HONO, OH, NO, and NO2 from the Lowest Lying Singlet and Triplet States in Ortho-Nitrophenol Photolysis, International Journal of Chemical Kinetics, 48, 785–795, https://doi.org/10.1002/kin.21033, https://onlinelibrary.wiley.com/doi/abs/10.1002/kin.21033, 2016.

Volkamer, R., Platt, U., and Wirtz, K.: Primary and secondary glyoxal formation from aromatics: Experimental evidence for the bicycloalkyl-radical pathway from benzene, toluene, and *p*-xylene, J. Phys. Chem. A, 105, 7865–7874, https://doi.org/10.1021/jp010152w, 2001.

Wallington, T. J., Ammann, M., Cox, R. A., Crowley, J. N., Herrmann, H., Jenkin, M. E., McNeill, V., Mellouki, A., Rossi, M. J., and Troe, J.: IUPAC Task group on atmospheric chemical kinetic data evaluation: Evaluated kinetic data, http://iupac.pole-ether.fr, 2018.

Warneck, P.: Chemistry of the Natural Atmosphere, second edition, Academic Press, 1999.

WMO: Air quality guidelines for Europe, Copenhagen: WHO Regional Office for Europe, 2000.

Yan, Y., Cabrera-Perez, D., Lin, J., Pozzer, A., Hu, L., Millet, D. B., Porter, W. C., and Lelieveld, J.: Global tropospheric effects of aromatic chemistry with the SAPRC-11 mechanism implemented in GEOS-Chem version 9-02, Geosci. Model Dev., 12, 111–130, https://doi.org/10.5194/gmd-12-111-2019, 2019.

https://doi.org/10.5194/acp-2020-461
Preprint. Discussion started: 2 June 2020

Atmospheric Chemistry and Physics Discussions

Young, P. J., Naik, V., Fiore, A. M., Gaudel, A., Guo, J., Lin, M., Neu, J., Parrish, D., Reider, H., Schnell, J., et al.: Tropospheric Ozone Assessment Report: Assessment of global-scale model performance for global and regional ozone distributions, variability, and trends, Elementa: Science of the Anthropocene, 6, 2018.